JTTEE5 17:181–198
DOI: 10.1007/s11666-008-9163-7
1059-9630/$19.00 © ASM International

Room Temperature Impact Consolidation (RTIC) of Fine Ceramic Powder by Aerosol Deposition Method and Applications to Microdevices

Jun Akedo

(Submitted March 25, 2007; in revised form December 18, 2007)

Ceramic integration technology requires downsizing and/or improvement of device performance in many applications, such as in the fabrication of microelectromechanical systems, display devises, fuel cells, optical devices, and RF components. For these applications, realization of high-speed deposition rate, low process temperature, and fine patterning in ceramic coating are very important. The aerosol deposition (AD) method has many advantages for above requirements in comparison with conventional thin-film method or thermal spray coating technology. In this article, advantages of the AD method are highlighted by realizing a comparison with conventional thin-film methods and thermal spray technology. Challenges associated with AD method are also highlighted. At the end, examples of integration of AD method in the fabrication of electronic components are also given to show the easiness in usage and in integration of this method in the device process flow.

Keywords aerosol, coating, cold spray, ceramic, deposition, impact, MEMS, optical device, pattern, RF component, consolidation

1. Introduction

The manufacturing of ceramics usually requires sintering at temperatures higher than 1000 °C which makes it difficult to compound or integrate ceramics with low-melting point, metals, glass, or plastics. This is a serious problem for upgrading electro-ceramic components and optical components. For example, an effective and reliable technology is required to fabricate actuators made of piezoelectric thick films for optical scanners, micromotors (Ref 1, 2), scanning force microscopy (Ref 3), micropumps, ultrasonic mixers (Ref 4, 5), and micromanipulators for medical applications in microelectromechanical systems (MEMS). Improvements in technological process will be very important in the near future to produce ink-jet printer heads that will reduce the printing time, and to produce flapper-actuators that will control the high-speed positioning of recording heads for high-density storage drives (Ref. 6). For these applications, using piezoelectric or electrostrictive materials with large strain and high-speed response often require dense and thick micropatterned films, thickness exceeding 5 μm in many cases (Ref 2, 7, 8). However, thick layers produced by conventional thin or thick film methods usually have cracks and may easily peel from the substrates. With these methods is also difficult to produce complicate material compositions and fabrication can be time-consuming and costly.

Figure 1 summarizes the conventional methods used to fabricate lead-zirconate-titanate ($Pb(Zr_{0.52},Ti_{0.48})O_3$, PZT) films on substrates and the applications of these films. There are many reports on the fabrication of PZT films of thicknesses ranging from 0.08 to 5 μm by sol-gel (Ref 9, 10), sputtering (Ref 11, 12) metalorganic chemical vapor deposition (MO-CVD) (Ref 13), pulse laser ablation (Ref 14), electron beam evaporation (Ref 15), and ion-beam deposition (Ref 16). In these methods, dense PZT film can be formed and oriented on a Pt/Ti/SiO_2/Si substrate. However, fabrication of PZT films with a thickness of over 1-3 μm using these methods requires much attention because there are many problems to overcome regarding film quality or deposition. Hydrothermal synthesis (Ref 17, 18) has the advantage of a low-process temperature at 150 °C and the poling procedure is not required. However, the surface roughness and the density of the films are poor. The PZT thick films fabricated by the screen-printing method (Ref 19, 20) have a low density and PZT/Pt/Si structures can be damaged because of the long firing time at temperatures higher than 800 °C. An improved screen-printing method with a low-temperature sintering and a high-resistance electrode has been reported (Ref 21), but the piezoelectric properties of films produced by this method were not reported. For sputtered and sol-gel derived PZT thin films, a postdeposition rapid thermal annealing treatment

Jun Akedo, National Institute of Advanced Industrial Science and Technology, Tsukuba, Ibaraki, Japan. Contact e-mail: akedo-j@aist.go.jp.

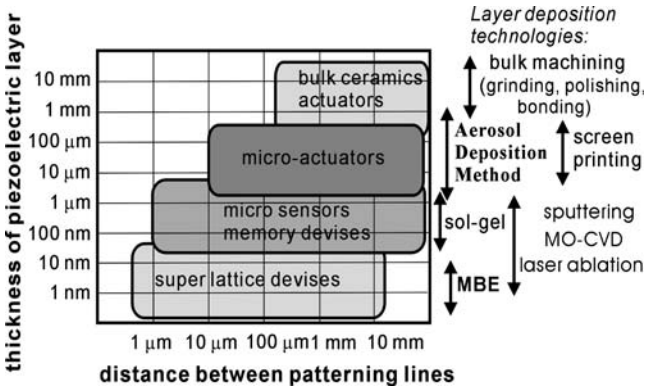

Fig. 1 Fabrication method for PZT layer in various thickness ranges

(Ref 22) was introduced to reduce the damage to the substrate or structure, and to improve the electrical properties. However, for thick films, with a thickness over 1 μm, this process was not so effective. The etching of thick ceramic films by plasma etching (Ref 23), inductively coupling plasma etching (Ref 24, 25), or reactive ion etching (Ref 26) is also difficult. For bulk PZT adhered to a Si membrane, it is difficult to ensure an adequate mechanical and electrical coupling between the films and to assemble complex structure. Thus, it can be concluded that, by conventional methods, fine patterning of thick (over 1 μm) PZT films on Si-based substrates is still difficult to realize.

To reduce costs and fabrication time and to avoid damages on circuitry already present on the substrate, it is very important to have a high-speed deposition rate, a low-process temperature, and fine patterning. Until now, a number of studies have been aimed at reducing the sintering temperature for the purpose of reducing energy consumption, and implementing innovative functional components through the integration with metal or glass materials. Several deposition methods based on the principle of particle collisions have already been investigated. Recently, cold spaying method (CSM) for metal materials has attracted much attention. However, for ceramic materials this method is not successful.

For these reasons, a new deposition technique based on collision adhesion of fine particles for fabrication and micropatterning of thick ceramic layers has been developed, named the aerosol deposition (AD) method. The AD (Ref 27-31) is a novel and a very attractive coating method for ceramic integration. Submicrometer ceramic powder is mixed with a carrier gas to form an aerosol flow, ejected through a micro-orifice nozzle and deposited onto a substrate in the deposition chamber kept under vacuum during the deposition. A special attention is paid to the character of primary powder particles and the deposition conditions. Using this method, ceramic layers of $Pb(Zr,Ti)O_3$, α-Al_2O_3, Y_2O_3, YSZ, AlN, MgB_2, and other ceramic materials with nanocrystalline structure, high transparency, high hardness, and high-breakdown voltage were formed at room temperature. It is suggested that during impact of the fine particles with the substrate, a part of the particle's kinetic energy is converted into a bonding energy between the substrate and the fine particles and between the fine particles themselves. In fabrication of thick films with thickness range of 1-100 μm, AD method has many advantages in comparison with conventional thin or thick film methods or thermal spray methods.

2. Aerosol Deposition Method

The AD method is based on shock-loading solidification due to the impact of ultrafine ceramic particles with a surface (Ref 27, 28). First, particles are mixed with a gas to generate an aerosol. This aerosol is ejected through a nozzle at low pressure and impacted onto a substrate to form a thin/thick film. During the impact with the substrate, part of the particle's kinetic energy is converted into thermal energy causing increase in temperature at the point-of-impact and promoting bonding between the substrate and the particles and also between multiple particles. However, the detailed mechanism occurring during the particle impingement with a surface in the AD method has not been fully clarified yet.

Figure 2 shows the deposition apparatus and Table 1 gives the deposition conditions for the AD method. The AD apparatus consists of two vacuum chambers connected by a tube. The first chamber is an aerosol-generation chamber and the second chamber is a deposition chamber. The deposition chamber is used for the formation and patterning of films. The aerosol-generation chamber has a carrier gas system and a vibration system to mix the powder with the carrier gas. The aerosol generated in this chamber is delivered to the deposition chamber by a pressure difference between the two chambers. The deposition chamber contains a nozzle, a substrate holder with a heating system, and a mask alignment system used for making patterned films. A rotary vacuum pump coupled to a mechanical booster pump is used to vacuum this chamber to a pressure of about 50-2000 Pa during deposition. Figure 2(b) shows various size deposition machines.

Sintered ceramic powders with a particle size range of about 0.08-2 μm are typically used as the deposition particles. After suspension in the carrier gas to form an aerosol, the aerosol is accelerated to several hundred m/s through a rectangular orifice with width <1 mm. Not all of the aerosol particles will be deposited onto the substrate. The ratio of deposited to nondeposited particles strongly depends on particle size and the degree of aggregation of the particles. To form films with an acceptable density and material properties, particles with a particular size and morphology must be used. To generate a jet of particles with acceptable size and morphology, a de-agglomeration device and a filter are used between the aerosol-generation and deposition chamber to break the particles apart as much as possible and to select particles in a prescribed size range.

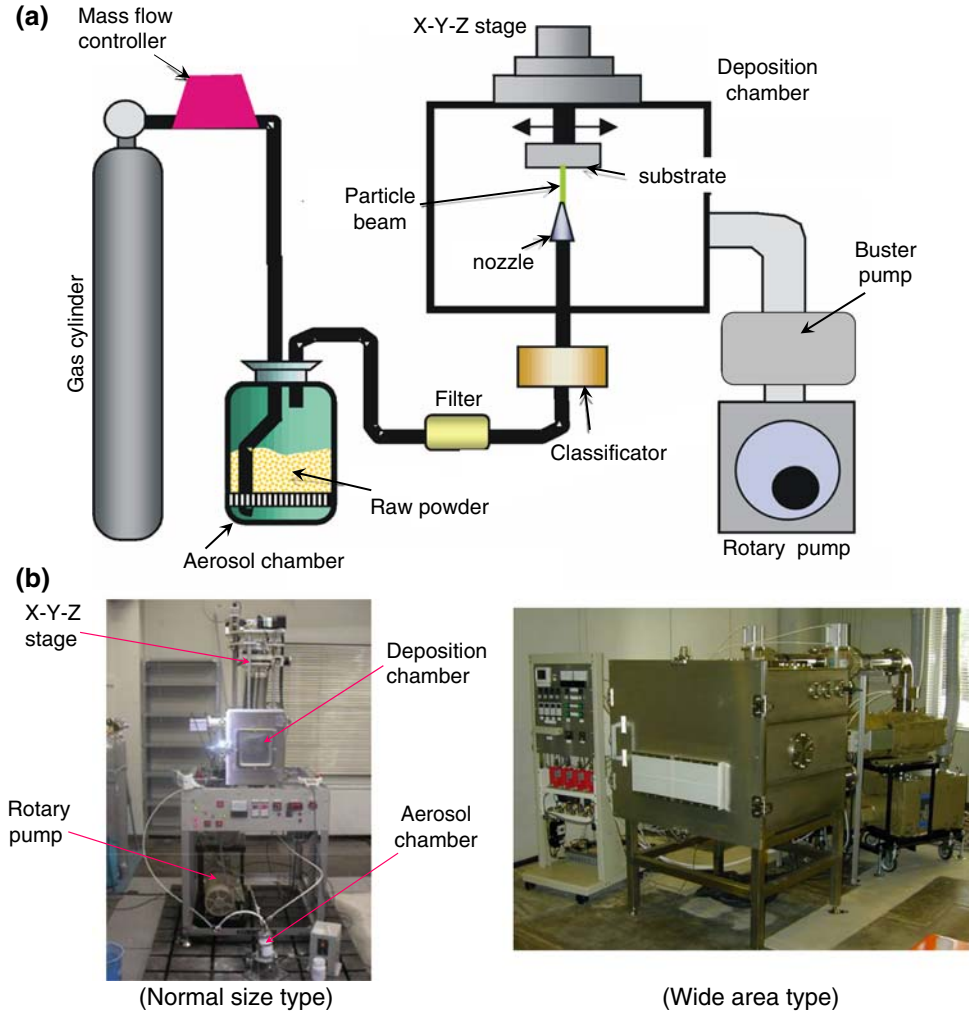

Fig. 2 Schematic (a) and prototype photograph (b) of aerosol deposition (AD) apparatus

Table 1 Typical deposition conditions (Experimental parameters)

Pressure in deposition chamber	0.05-2 kPa
Pressure in aerosol chamber	10-80 kPa
Size of nozzle orifice	5×0.3 mm^2; 10×0.4 mm^2
Accelerating gas	He, N_2, air,
Consumption of accelerating gas	1-10 l/min
Maintained substrate temperature during deposition	300 K
Scanning area (area of deposition)	40×40 mm^2, 400×400 mm^2
Scanning speed of the nozzle motion along substrate	0.125-10 mm/s
Distance between the nozzle and substrate	1-40 mm

3. Room Temperature Impact Consolidation

3.1 Consolidation of Ceramic Powders at Room Temperature

For the AD method, the high-speed film formation of ceramic films at room temperature with a high density and a high transparency is possible by optimizing the particle diameter and deposition conditions. The result is a process that yields an acceptable consolidation at room temperature without the need for a thermal treatment. This process is called room temperature impact consolidation (RTIC) (Ref 28, 29, 32).

Figures 3 and 4 show micrographs of typical RTIC ceramic layers, cross-sectional SEM image of an as-deposited α-Al_2O_3 layer at room temperature, comparison of its x-ray diffraction (XRD) profile with the profiles obtained for the raw powder and bulk material, and Transmission Electron Microscopy (TEM) images of as-deposited layer and starting powder. The formation of thick films with a thickness over 100 μm having high transparency were confirmed, as shown in Fig. 3(a) and (b). Using a multinozzle system, the coating area could be enlarged as shown in Fig. 3(c). The aerosol deposited films showed a relatively good thickness uniformity of 1.4%. The surface roughness (Ra) was <100 nm. The deposited film has a high density and randomly oriented polycrystalline nanostructure with a crystal grains smaller than 20 nm in length. TEM and electron diffraction imaging did

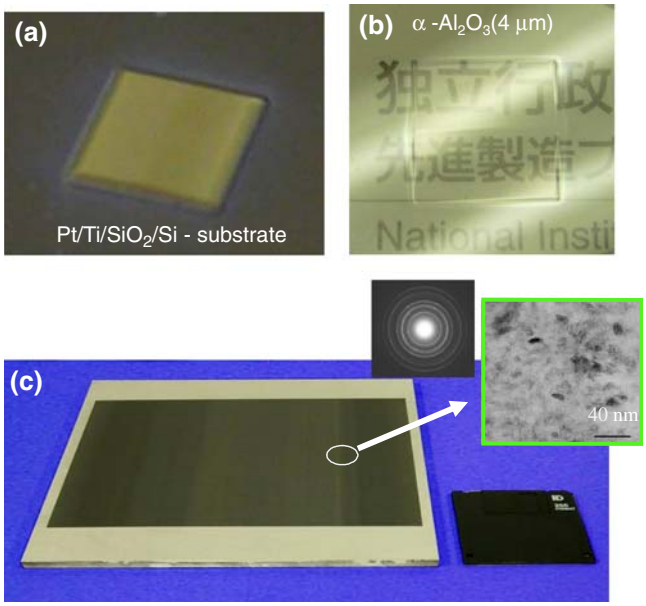

Fig. 3 Photograph of AD-ceramic layer deposited at room temperature using RTIC phenomenon. (a) Thick ceramic layer: over 500 mm; (b) transparent ceramic layer: 99% @ 400-900 nm; and (c) wide area coating: 200 × 200 mm^2

not show either amorphous layers or hetero structures at the boundary of the crystal grains. The XRD profiles confirmed that the spectral phases of the α-Al_2O_3 particles were retained in the deposited layer. However, a broadening of the spectral peaks and a slight shift in peaks angle positions were observed. The reason for the change between the spectra of the raw particles and the deposited layer is due to the reduction of the film crystal size and/or the distortion during the deposition. Clear lattice images in crystal grains <10 nm were observed, as well as uniform microstructures at the boundary between the substrate and the deposited layer. For α-Al_2O_3 layers deposited at room temperature, the film density was over 95% of the theoretical density and Vickers hardness was 1600 HV (Ref 27). Such α-Al_2O_3 layers are acceptable for use as abrasion-resistant coatings (Ref 30). The crystal grain size of the as-deposited films was smaller than that of the starting particles because the starting particles break down during collisions.

Table 2 shows the relationship between Micro Vickers hardness, the crystallite size and particle impact velocity in various AD-deposited materials. The layer hardness increased with increasing particle-impact velocity, and sometimes was higher than that of the bulk material, which was sintered at a high temperature. Critical particle velocities for an acceptable RTIC ranged from 150 to 500 m/s, and the velocity needed to create films with acceptable hardness tended to increase with increasing sintering temperature for a particular ceramic material.

Although distortions were included inside the films, a rise of the substrate temperature due to particle collisions was not observed. Consolidation of ceramic powders was possible at room temperature without the use of binders. Even if the formation of thin films using RTIC does not require sintering, it produces high-density films. Acceptable room-temperature deposition was observed not only for oxide materials such as α-Al_2O_3, lead-zirconate-titanate (PZT: $Pb(Zr_{52},Ti_{48})O_3$), and Ni-Zn-Fe_3O_4, but also for non-oxide materials such as AlN and MgB_2. In either case, particles with diameter greater than 80 nm are needed to make films having an acceptable hardness.

3.2 Impact Particle Velocity and Local Temperature Increase during AD Process

The particle's velocity during the AD method was measured by a time-of-flight method, in which some part of the particles flow was mechanically cut from the total flow and deposited onto a moving substrate. The deflection of the deposited pattern from the center axis, the geometrical dimensions and the moving substrate speed provide data to determine the particle flow velocity (Ref 31). The merit of this method is that the impact particle velocity is directly measured. This is a more accurate method than the conventional measurement using a high-speed camera that can only estimate particle flow velocity. Figure 5 shows the relationship between the impact particle velocity and gas consumption in controlling the particle velocity. The particle impact velocities were estimated as varying from 150 to 500 m/s. The critical velocity for RTIC of α-Al_2O_3 was 150 m/s. This implies a very small kinetic energy compared to that detained in the conventional shock compaction process. Using the values measured for particle impact velocity, the local rise in temperature and the shock pressure at the point of impact between the particle and the substrate were simulated by finite-element method (FEM) computational simulations using AUTODYNs-2D (CRC Solutions Co., Tokyo, Japan) with Johnson-Holmquist material model (Ref 29, 33, 34). In the simulation, the particle diameter was set to 0.3 μm, which was the same as the average diameter of the starting α-Al_2O_3 powder. Bulk material constants of α-Al_2O_3 (Ref 35) were used for these simulations. The maximum local temperature rise and the shock pressure at the point of impact during layer formation does not exceed 500 °C and 2.5 GPa, as shown in Fig. 6(a) and (b). This local increase in temperature is too small to induce any ceramic sintering. Consolidation features of ceramic material fabricated using the AD method are fundamentally similar to those in the case of the shock compaction method. However, the local rise in temperature and the compact pressure for brittle materials such as ceramics and glasses were less than those of over 1000 °C and 10 GPa that are typical for conventional shock wave synthesis (Ref 36, 37).

3.3 Densification Mechanism of Ceramic Layers in AD Process

From the simulation and experimental results, it may be concluded that particle partial or total melting does not occur during collision. Then, how can the reduction of the crystallite size for the starting particle and the production of dense structures during deposition be explained?

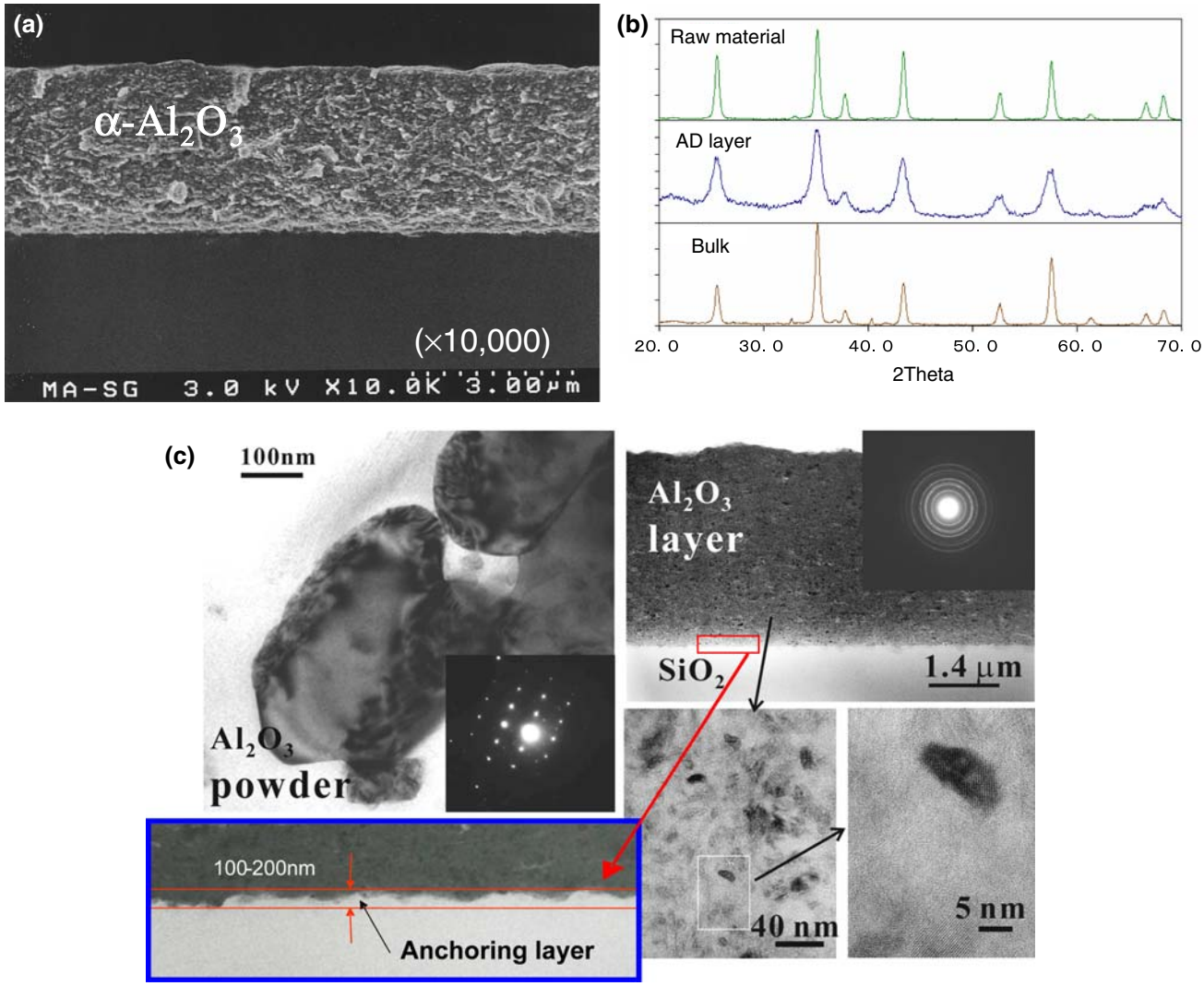

Fig. 4 Microstructure of α-Al_2O_3 layer deposited at room temperature by AD method. (a) cross-sectional SEM image of as-deposited layer at R.T.; (b) comparison of XRD profiles; (c) TEM images of starting powder and as-deposited layer at R.T

Table 2 Mechanical properties of as-deposited AD layers

Material	Hardness (Hv)		Average crystallite size of the layer (nm)	Particle velocity at the collision (m/s)
	Layer (deposited at R.T.)	Bulk (a)		
Oxide				
A-Al_2O_3	1200-2100	1900 ± 100	13-20	150-500
PZT	400-550	350 ± 50	10-30	100-300
(Ni,Zn)Fe_2O_3	700-750	1040 ± 80	5-20	250-600
Non-oxide				
AlN	1100-1470	1180 ± 90	5-15	200-600
MgB_2	700	···	5-20	300-550

(a) Bulk sample were prepared from the same starting powder as layers, by conventional sintering procedure (at temperature over 1200 °C)

There are two possible explanations:

(i) First, only small particles <20 nm in the jet flow will actually take part at the deposition to form the layer, and/or

(ii) Second, fracture and deformation of starting particles are obtained during the impact with the substrate to fill up the gaps between the deposited particles.

To clarify this, a mixed aerosol of α-Al_2O_3 and PZT powders was deposited to form a composite layer. The cross section of this layer was observed by HR-TEM to investigate the densification and bonding mechanism of ceramic particles. Figure 7(a) and (b) shows TEM images of the α-Al_2O_3/PZT composite layers. Selected area diffraction (SAD) for both starting particles indicates that these particles have a single crystal structure. Black and white regions indicate PZT and(α-Al_2O_3, respectively, because lead elements are

much heavier than aluminum elements and the electron absorption for each element depends on their mass. A laminar structure along the substrate plane was only observed in the cross section TEM image. Inside black and white regions, electron diffraction patterns with an 80 nm electron beam irradiating diameter indicate a typical net-pattern image, as shown in Fig. 7(b), and randomly oriented small crystallite <20 nm were observed in a zoom-up image. These crystallites were almost the same in size as those in the as-deposited α-Al_2O_3 films (shown in Fig. 4c). The volume of the black part, assuming an oval shape, was close to that of starting particles of PZT. The fracture toughness of the α-Al_2O_3 starting particle was estimated as 3-6.5 GPa by the special nano-indentation system (Ref 38). This value was close to the value obtained for maximum impact pressure in the simulation meaning that the α-Al_2O_3 starting particle is most likely to be fractured during impaction. From these results, it was concluded that the dense structure occurs due to the reduction of crystallite size by fracture or plastic deformation at room temperature during the AD process. This explanation for densification of ceramic particles during the AD process is different from that of conventional shock compaction. The plastic deformation of ceramic particles at room temperature can be assumed not only for α-Al_2O_3 case and may be a general phenomenon because AD layers for a large variety of ceramic material could be easily formed.

By comparison, the Cold Spray (CS) method (Ref 39, 40) for metal coating requires particle velocities over 500 m/s to fabricate high-density layers, being much higher than the ones required for AD method. Also, melting points of ceramic materials are higher than that of metal materials and ceramics are more difficult to deform. Therefore, the bonding mechanism in the case of AD cannot be explained as for the case of the CS method. To date, the bonding mechanism between the fine particles themselves and between the substrate and the fine particles has not been clarified. There are still some questions to be answered regarding the AD deposition. Does the generation of a clean and active layer of starting particles makes the particle bonding at a low temperature possible? Is some kind of chemical reaction induced during impaction? To answer these questions more studies are needed on the bonding mechanism of ceramic particles during the AD deposition.

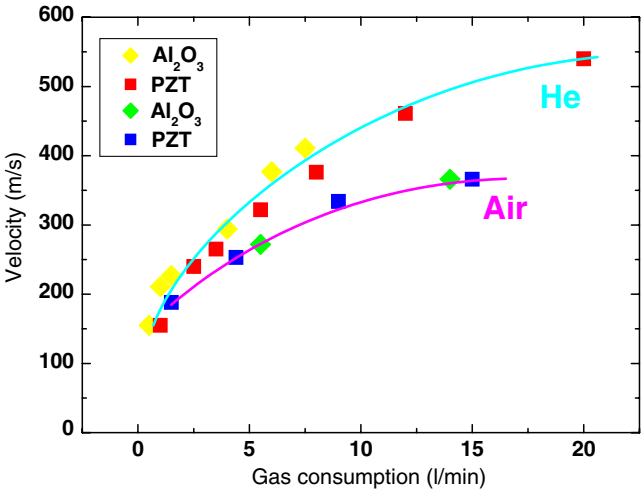

Fig. 5 Relationship between impact particle velocity and gas consumption to control the particle velocity for different gases (nozzle of 10 × 0.4 mm^2)

3.4 Influence of Carrier Gas

If the carrier gas and pressure in the deposition chamber are properly selected to reduce the electrical discharge during the particle deposition, transparent PZT and alumina films with transmission efficiencies of 60-90% at wavelengths ranging from 400 to 800 nm can be formed at room temperature (Ref 29, 32). The reason why this can be achieved is because during deposition the size of the defects (pores, grain boundaries) in the starting particles is reduced being smaller than those found in sintered, bulk materials, and because the particle grain size is smaller than the wavelength of the visible light. Carrier gas and gas flow seem to have an effect over the AD films optical properties. Plasma illuminations have been observed

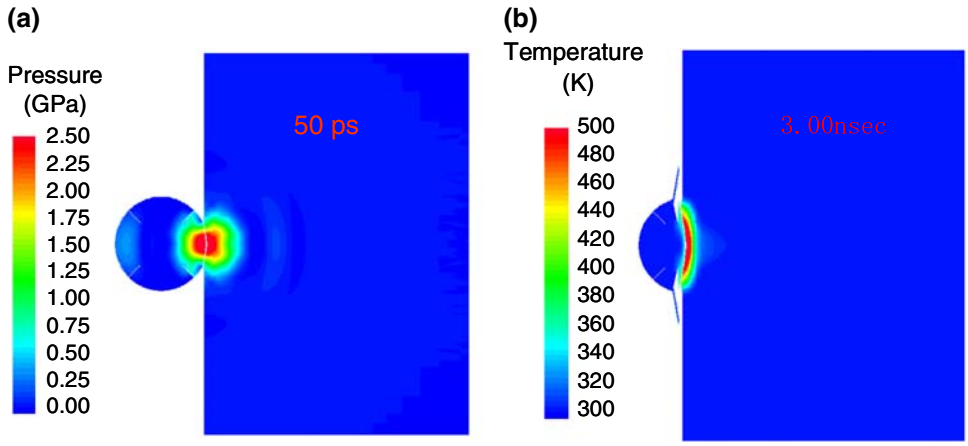

Fig. 6 FEM simulation of the local rise in temperature and shock pressure during impact of particle with the substrate for AD deposition. Impact particle velocity was 300 m/s (Ref 29)

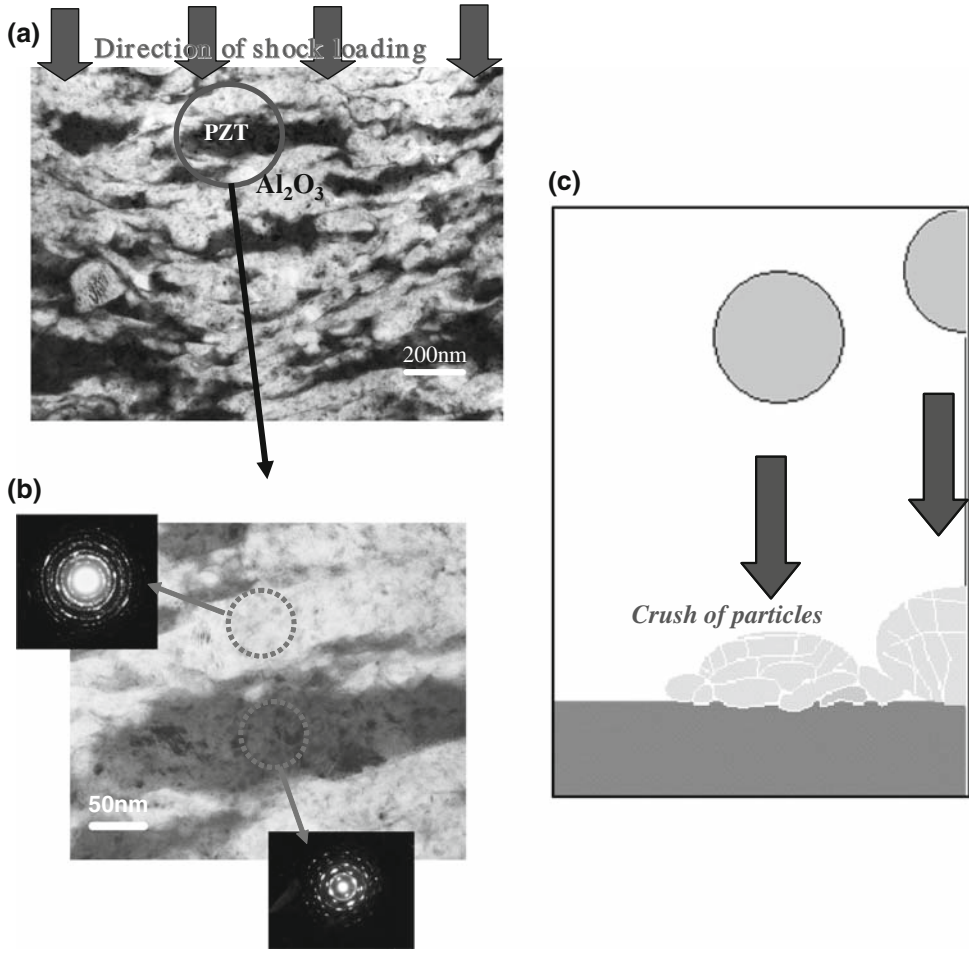

Fig. 7 TEM image α-Al_2O_3/PZT composite layer and densification mechanism. (a) Cross-sectional TEM image; (b) zoom up image; and (c) densification image (Ref 29)

during collision of fine particles with the substrate due to the fracture of brittle materials (Ref 41). Photographs of PZT films deposited at room temperature using He or N_2 as carrier gas and the emission spectra at the point-of-impact are shown in Fig. 8. The color of the deposited films is influenced by the carrier gas. Considering previous reports (Ref 28, 29), the film color change is explained by discharging during the deposition. Such discharging induces defects in the film and the drastic decrease of the films transmittance. When He gas has been used, if consumption was increased, plasma discharging was increased and thus the film color became even darker. The results of the emission investigation will be reported in detail later.

4. Deposition Properties and Film Patterning

4.1 Deposition Ratio and Influence of Starting Powder Properties

High-deposition rates can be achieved easily with AD method because the source material is already in particle state form. These deposition rates are at least 30 times higher than other conventional thin-film formation methods. Therefore, the AD method is an attractive manufacturing process due to high throughput. The particle velocity and concentration in the aerosol jet at the nozzle increases with increasing carrier gas flow rate, resulting in increased deposition efficiency. Starting particle properties, such as the average particle size and the size distribution, mechanical, and surface properties can also strongly affect the deposition efficiency (Ref 42).

The deposition rates for PZT AD layers using powders subjected to various milling procedures are indicated in Fig. 9. It can be seen that, by increasing the milling time, the deposition rate of the PZT layer significantly increased and reached a maximum of 73 μm/min for a 5 mm^2 deposition area when powder was milled for 5 h. This value is 30 times higher than that for a starting powder without the milling procedure. An interesting fact is that the deposition rate decreased as a result of further milling to 30 h. It is assumed that particle surface properties (for example, surface activation, defects, and gas absorption) will change by longtime milling making them less probable to be deposited in the same conditions. This milling

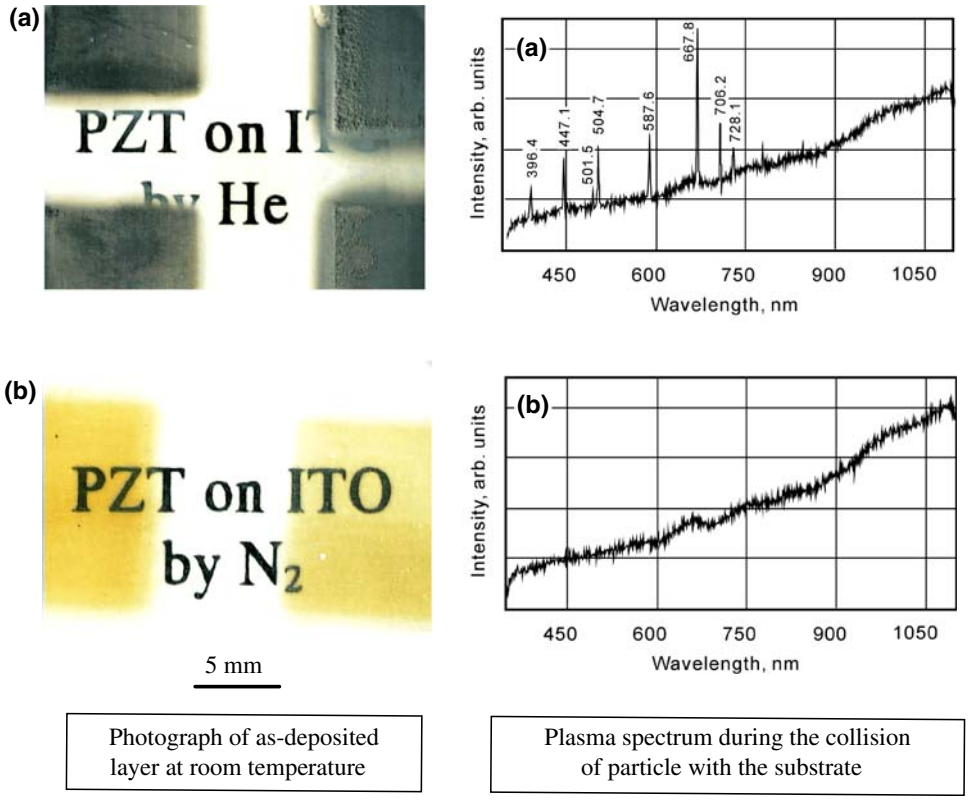

Fig. 8 Influence of carrier gas to the transparency of as-deposited layers (Ref 32) (a) He gas and (b) N_2 gas

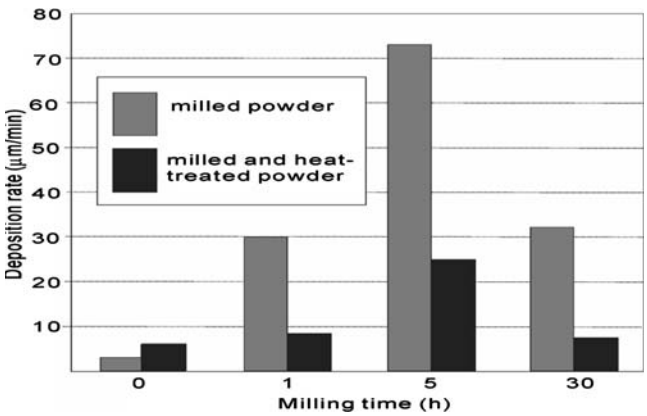

Fig. 9 Deposition rate for PZT film formation at room temperature using powder milled for different duration times with (*black bar*)/without (*gray bar*) heat-treatment procedure at 800 °C for 4 h in air (Ref 42)

procedure is applicable to control the porosity of ceramic layers deposited by the AD method.

The starting powder particle size and shape strongly influence the RTIC phenomenon in the AD method. If spherical α-Al_2O_3 ultra-fine particles with average particle size around 50 nm were used, after AD deposition the films have a pressed-like structure and the RTIC phenomenon could not be observed even if the ejecting particle velocity from the nozzle was over 400 m/s and particle size was very small (Fig. 10a). In contrast, if nonspherical α-Al_2O_3 fine powder with average particle size around 1 μm was used, the deposited particles on the substrate were consolidated at room temperature and RTIC phenomenon was observed even for particle velocities around 200 m/s, as shown in Fig. 10(b). As a result, high density and transparent ceramic layers were obtained. These results are explained by aerodynamic properties of the particle jet flow near the substrate. If particle size and weight are too small, the particle follows the carrier gas flow as shown schematically in Fig. 11. Therefore, the particle velocity normal to the substrate is largely decreased and is not high enough to obtain RTIC phenomenon. A more detailed investigation about the particles aerodynamic properties in the AD method is still needed to be conducted.

An advantage of AD method over conventional thin film and thermal spray coating methods is that substrate surface does not need precleaning to achieve good deposition. During the initial deposition stage, the particles impacting the substrate will act as cleaning agents in a similar way as in sand-blasting processes. Surface contaminants such as dirt and oils are removed by the initial particle collisions. The deposition automatically begins when the surface becomes sufficiently clean. The film adhesion strength to glass and metal substrates may be in excess of 30 MPa, because anchoring layer having a

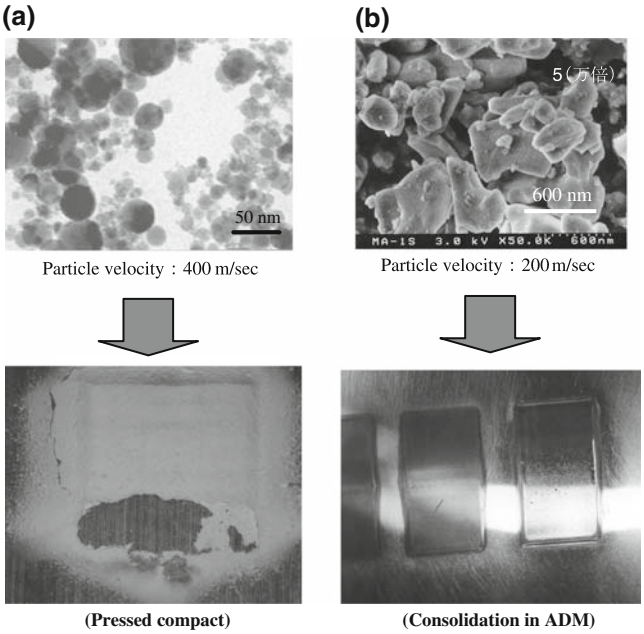

Fig. 10 Influence of starting particle diameter for RTIC phenomenon on AD method. (a) Average diameter: 50 nm and (b) average diameter: 700 nm

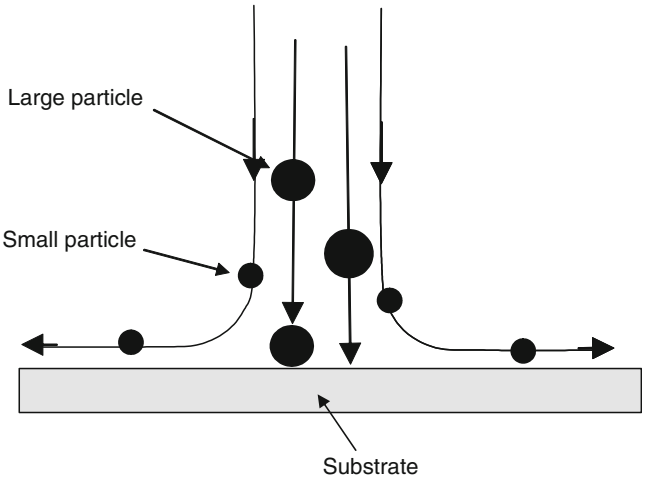

Fig. 11 Particle trajectories in an aerosol jet flow near substrate on AD method

thickness of about 100-200 nm was formed in the interface between the substrate and the deposited layer. To obtain maximum adhesive strength, a substrate with suitable hardness and elasticity is needed to allow the formation of the anchoring layer. A substrate that is very soft will be etched by the particle jet flow and the deposition will not occur. On the other hand, when a substrate with large hardness value is used the adhesion strength between the deposited layer and substrate is weak and the film may easily peel-off.

4.2 Patterning Properties of Ceramic Film

Ceramic film patterning can be achieved by using a mask deposition method, in which a particle jet is impacted onto the substrate through a defined pattern mask that contains openings with width of at least 50 μm. In this case, it is important to consider the aerosol jet flow in the deposition chamber and through the mask orifices. If the pressure in the deposition chamber is not sufficiently low, the particle jet is scattered by the edge of the openings in the mask and the resulting mask pattern is not preserved on the substrate.

The effect of the ceramic particles sprayed onto a substrate change from deposition to erosion (Ref 43), as shown in Fig. 12, depending on the particle diameter, velocity, and angle of incidence, β, of the particle jet to the substrate. In the figure, β_c is the angle of incidence when deposition rate and abrasion rate have the same value, and the normalized thickness is the thickness of the PZT layer after AD deposition relative to the initial value of PZT thickness. These factors also influence the layer density and surface roughness. However, to achieve acceptable patterns through a mask with acceptable detail the angle of incidence of the particle jet must be kept within a specified range. This is because the angle of incidence affects the flow patterns on the downstream side of the mask, which in turn affects the deposition efficiency and the degree to which the mask profile is distorted. Figure 13 shows a thick, patterned PZT layer deposited under optimum deposition conditions onto Si, SUS, and Pt/Si substrates (Ref 44). A ceramic microstructure with a 50-μm line width and aspect ratio (line height/line width) >1 can be patterned by controlling the substrate heating temperature and starting particle properties. The AD method is useful for making piezoelectric films more than 10(μm thick, for applications such as ultrasonic devices. However, the pattern width <50 μm were difficult to obtain. Recently, the production of ceramic fine patterns using AD method and lift-off process was tried. The hardness and thickness of the photo resist layer was chosen carefully. As a result, a minimum pattern width <10 μm for a 2 μm thick PZT and α-Al_2O_3 layers were obtained, as shown in Fig. 14.

5. Other Similar Methods and Comparison with the AD Method

5.1 Coating Process Based on Collision of Solid State Particles

Several deposition methods based on the principle of solid state particles collision have already been investigated. From previous studies, particle deposition in the AD method strongly depends on the particles diameter and velocity**.** Figure 15 shows a comparison between AD method and other deposition methods based on collision of solid state particles according to the particle diameter and velocity. The deposition methods can be classified in two, depending on the type of particle acceleration:

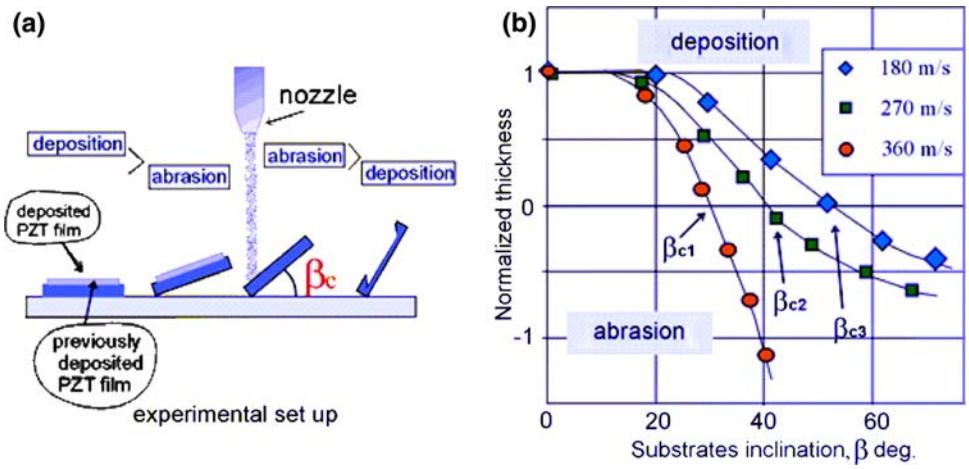

Fig. 12 Particle jet flow angle of incidence effect to deposition properties (Ref 43)

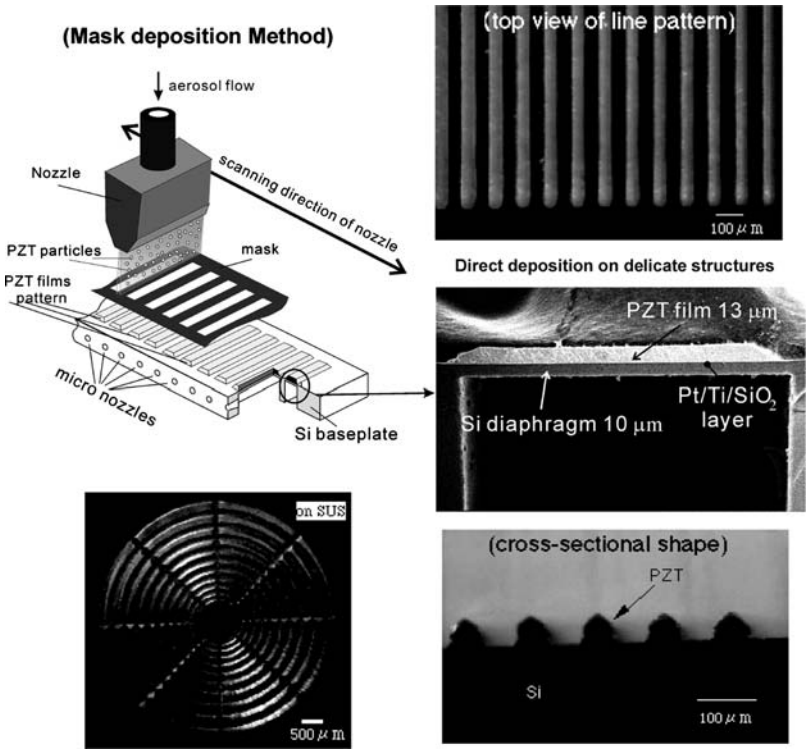

Fig. 13 Patterning properties of thick ceramic layers on AD method using mask deposition method

(i) acceleration by electric filed (electrostatic particle-impact deposition, EPID method (Ref 45) and Macron Beam method (Ref 46)) and (ii) acceleration by gas transportation (CS method, Ref 47; GD method, Ref 48; and AD method). For all these methods, the formation of the thin/thick films is based on the acceleration of small particles and their impacts with the substrate. The EPID process was the precursor of the coating technologies using electrical field acceleration of ultrafine particles and was originally developed by Ide et al. (Ref 49). The gas deposition (GD) method (Ref 50) is a coating technology of ultrafine particles via acceleration by mixing with high-speed carrier gas flow and was originally developed in ERATO Hayashi UFP-Project in Japan. Cold Spray method (Ref 39, 40) was developed by Anatolii Papyrin at the Institute of Theoretical and Applied Mechanics of the Russian Academy for producing metallic thick coatings. The hypersonic plasma particle deposition (HPPD) was

originally developed at Minnesota University (Ref 51) for Si, SiC, and ceramics thick coatings. The supersonic cluster beam deposition (SCBD) method (Ref 52) was not included here, because the cluster size was about 10^3 atoms and collision phenomenon was slightly different from that in collision of fine or ultrafine particles.

Generally, in these coating methods, it is considered that the kinetic energy of the fine particles is released at the impact during the very short collision time, which is <1 μs, residing in an increase of the surface temperature of particles at the contact area above the melting point

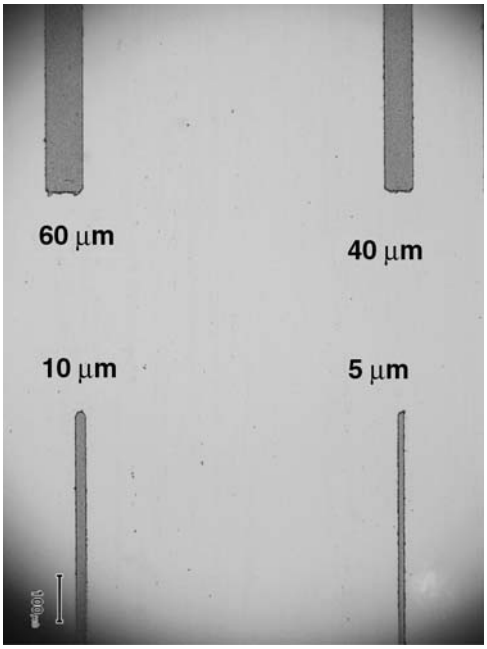

Fig. 14 Fine patterning of ceramic layers deposited by AD method using lift-off process with photo-resist

helping particle to bond to the surface (Ref 49, 50). However, it has been observed that the particles bondage is almost realized in solid state form. The principles of these methods are completely different from that of the conventional thermal spray method, which need melting or partial melting of the starting particles to make particles bond. In addition, it is not clear whether the bonding state between particles in fine particle layers formed by each technique is the same. There are few reports about the mechanism of energy conversion during a particle collision with a substrate, but we suspect that some differences in the deposition mechanisms between these methods exist.

The EPID method is more appropriate for conductive material due to the necessity of charging up the particles. Thick film formation (over 1 μm) with EPID method has not been reported yet (Ref 49). It is believed that ultrafine particles could be imbedded partially in the substrate at the time of collision and a mixed layer consisting of particles and the substrate materials is formed. It is also believed that layer growth for this method is low because of weak bonding between the jet particles. For the GD method, metallic and ceramic ultrafine particles having a diameter <100 nm and a highly activated surface are used. These ultrafine particles are formed by the condensation of an evaporated metal under high-pressure conditions in a vacuum chamber. In HPPD method, active ultrafine particles are also used and these particles are produced under a high-pressure condition after the condensation from the gas phase in the nozzle. Deposition properties in the HPPD method and the SCBD method show the same tendency as that in the GD method as reported in Ref 51 and 52. Deposition efficiency of the EPID method seems very low. On the other hand, the GD method, the CS method and the HPPD method have high-deposition rates. In the case of the CS method, large size particles with a diameter over 10 μm are accelerated by hot carrier gas at 300-600 °C and sprayed on a substrate under

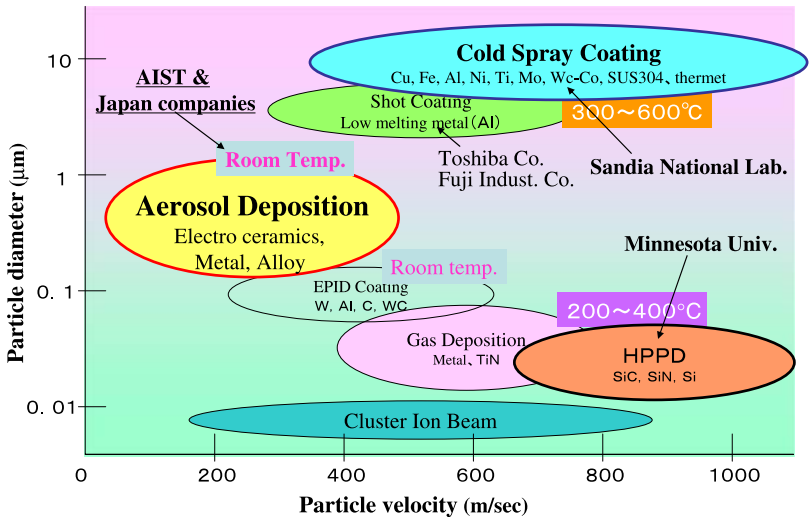

Fig. 15 Comparison between AD method and other methods based on collision of solid state particles

atmospheric condition using ultrasonic nozzle (Laval Nozzle). This method is very similar to the AD method and the conventional thermal spray coating process, but producing ceramic coatings has not been successful so far.

5.2 Comparison between AD method and other methods

The GD method enables the formation of metallic nano-crystal layers at room temperature. However, the layer density is low ranging between 50 and 80% of that of the bulk material. To obtain a high-electrical conductivity comparable to that of bulk material, grain growth of deposited layer using a thermal heat treatment such as substrate heating or heating of carrier gas is necessary (Ref 50). In addition, a high-density layer structure and a high adhesion with a substrate were not obtained for impact velocities <500 m/s (Ref 31). With AD method and CS method, highly dense and hard layers having a thickness of several mm can be obtained with relative ease. In addition, these methods seem to be very practical methods due to the simplicity of device structure. But, for the CS method, the formation of ceramic layers was not reported at all, though there were many reports for the formation of metal and metal alloy layers. In addition, for low-melting point materials such as Al, Ni, or Cu, the particle impact velocity to obtain the formation of a coating, known as critical velocity, was very high, ranging between 500 and 700 m/s (Ref 39, 47). In contrast, high-temperature melting materials such as α-Al_2O_3 can be deposited at room temperature by the AD method. The particle impact velocity is low and ranging between 150 and 400 m/s as shown in Fig. 4. The deposition properties are different from that of the CS method. For the AD method, the kinetic energy, particle diameter and velocity of the particles are smaller than that in the CS method. These results can be explained by the fact that particle impact velocity on the CS method is reduced by the reflection the jet flow and by resistance of the air layer near the substrate in atmospheric conditions. As a result, impact velocity and pressure in the CS method are not enough to produce the RTIC phenomenon, though the particle velocity just after ejection from the nozzle is very high. It is believed that a critical particle mass is necessary to overcome the slow-down resistance by the atmospheric layer near the substrate. Therefore, no reports on the deposition of small particles having a diameter <5 μm with the CS method could be found. With the AD method, it is possible to deposit not only metallic materials, but also ceramic materials. It is believed that the AD method and the CS method have RTIC phenomenon for solid state particles as common principle, as both deposition conditions and microstructures are comparable in the reported papers. However, it has to be pointed out that the AD method is different from the CS method because RTIC conditions for these two methods are very different.

At the present state, the understanding of the deposition mechanisms due to the collision of solid state fine particles is insufficient. A more detailed understanding is necessary and will be needed in a near future.

6. Electrical Properties of AD films and Improvements by Heat Treatment

Fundamentally, the above-mentioned coating methods are based on the shock-loading consolidation of solid state particles with or without thermal or plasma energy assistance. The microstructures of the films produced by these methods are completely different from those of the films made by typical spray-coating methods, because the primary powders used are not melted before impact with the substrate and particles are directly bonded in their solid state. The expected features for these methods are a dense film formation at a low temperature and the retaining of the primary material composition and the crystal structure. However, there is no report about applications of these methods to electrical and functional materials. It should be mentioned that, if the crystal structure of the ceramic particles is retained during the deposition, the processes temperature might be decreased and the application of these methods are expected to spread to the electro-ceramics materials.

The AD layers deposited at room temperature generally have high-electrical insulation and electrical breakdown characteristics that exceed that of the bulk material. For example, the electrical breakdown of α-Al_2O_3 and Y_2O_3 exceeded 3 MV/cm and for PZT it was found to exceed 500 kV/cm (Ref 27, 53). The volume resistivity, the dielectric constant, and the dielectric loss of α-Al_2O_3 layer formed by AD method were 1.5×10^{15} Ω cm, 9.8 at 1 kHz and 0.2%, respectively (Ref 54). Those values are almost the same as those of the bulk material. Such electrical characteristics can be useful for developing devices such as electrostatic chucks (Ref 55), electrical insulation layers with a good thermal conductivity for high power electric devices.

Although PZT layers deposited at room temperature exhibit piezoelectric and ferroelectric behaviors, their properties are unacceptable for practical applications because of the structural defects introduced and the reduction of the crystallite size during deposition. By postannealing in air at temperatures ranging from 500 to 600 °C, a grain growth of fine crystals and a defect recovery in AD layers was observed, which dramatically improved the ferroelectric properties. The dielectric constant (ε) and the piezoelectric constant (d_{31}) of post-annealed layers formed at 600 °C were 800-1200 and −100 pm/V (Ref 56), respectively, which is comparable to the values obtained with conventional thin-film formation methods. Moreover, the electrical breakdown (<1 MV/cm) and the Young's modulus (>80 GPa) of the AD films exceeded those obtained with conventional thick film formation technologies. By postannealing at temperatures up to 850 °C, a remnant polarization (Pr) of 38 μC/cm^2 and a coercive field strengths (Ec) of 30 kV/cm were obtained in the PZT films (Ref 57, 58). Even without adding any special additives to the fed particles or using special procedures, compared to conventional screen-printing methods, the AD method permits a 300-400 °C reduction of the process temperature. For films deposited

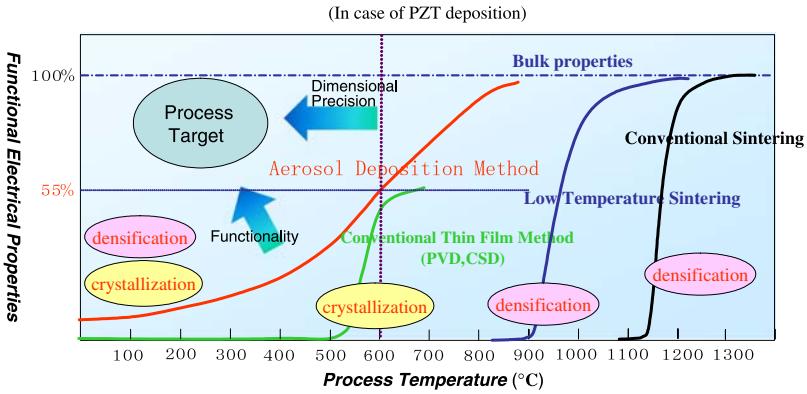

Fig. 16 Improvement of electrical properties of ferroelectric AD layers by heat treatment

using both conventional and AD methods, the effect of heat treatment on electrical properties of the films is shown in Fig. 16. For both conventional bulk and thin-film processes, heat treatments at more than 600 °C were required to obtain crystallization and densification of the films. The most important characteristic of the AD method is that, compared to the properties of films deposited using classic coating methods, the as-deposited film has a more dense and crystallized structure being close to the bulk material.

7. Device Application Developments

7.1 Piezoelectric Device Applications

Already microdevice applications such as MEMS optical scanner, ink jet head and ultrasonic motor have been developed using piezoelectric materials. Using the AD method, a high-performance optical microscanner with a scanning speed at a resonance frequency over 30 kHz and a scan angle (peak-to-peak value) over 30° in atmospheric environment was successfully fabricated by the deposition of the piezoelectric materials at a high rate onto the scanner structure fabricated by Si-micromachining or mechanical punching, as shown in Fig. 17 (Ref 59, 60). This optical scanner with a high-scanning speed is expected to be a key component for various types of sensor for the next generation of projection display devices. Further research is still under way targeting the realization of 3D displays and holographic data storages and the development of fast response spatial light modulators aiming to replace the liquid crystal technology. PZT-based Magneto-Optic Spatial Light Modulators (PZT-MOSLM) prototype, shown in Fig. 18, has been fabricated by incorporating a piezoelectric thick film into magneto-optic materials (Ref 61). In MOSLMs, the high-switching speed results from the fact that the pixel switching is achieved by switching the direction of magnetization, up or down within 1 ns. The novel MOSLM driven by an electric field instead of a magnetic field was first achieved by using the piezoelectric effect of AD-PZT thick films, which reduces the anisotropic energy of the structured garnet film. The pixels could be easily switched

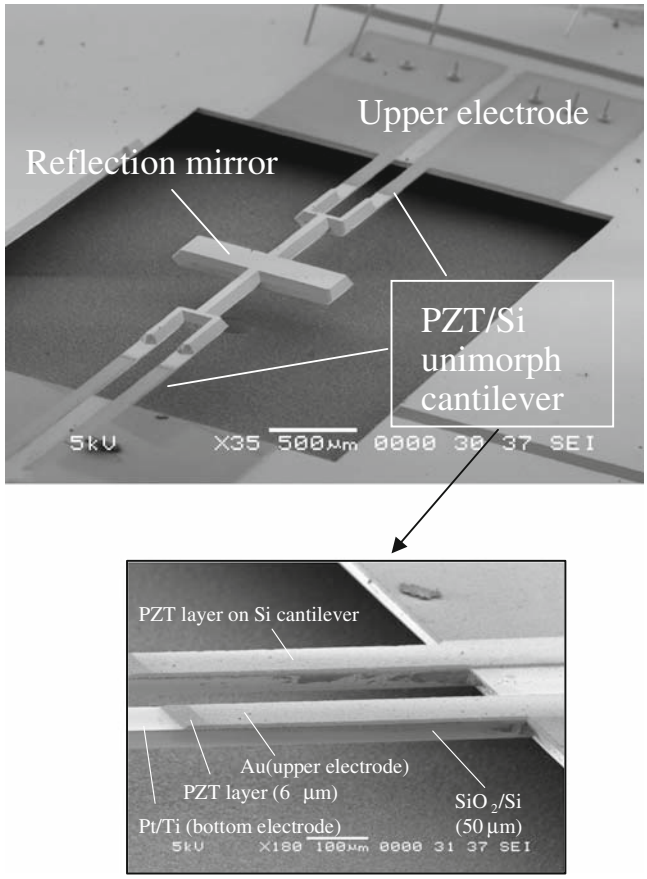

Fig. 17 Optical microscanner driven with PZT thick layer deposited on Si-MEMS structure by AD method. Scanning speed: over 30 kHz; scanning angle: over 30°

in the presence of a small external bias field. As a result, the power consumption of such MOSLM was drastically reduced being 10 times smaller than that of a conventional current driven type one. Successful pixel switching at 20 MHz has already been achieved with an 8 V drive voltage. Tube typed ultrasonic micromotors, shown in Fig. 19, were also fabricated as the prototype for the

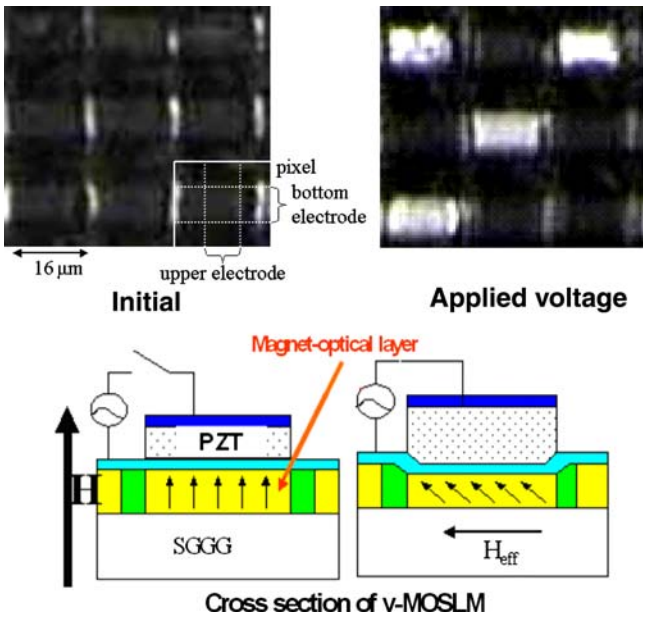

Fig. 18 PZT-based magneto-optic spatial light modulators driven with PZT thick layer deposited on Bi-YIG single crystal structure by AD method (Ref 61)

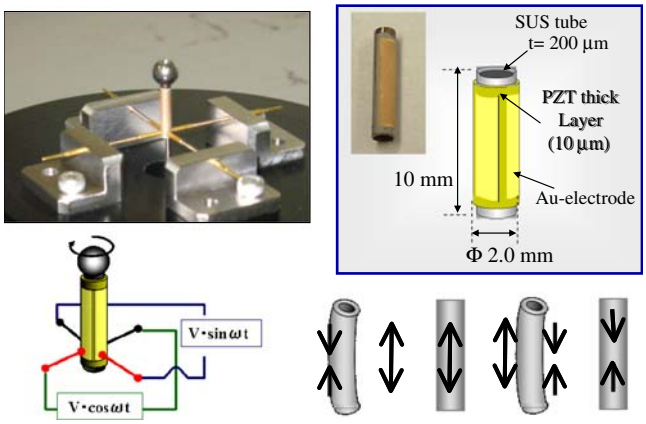

Fig. 19 Tube typed ultrasonic motor driven with PZT thick layer deposited on SUS tube by AD method

application of the AD method (Ref 62). In this device, a 10-μm PZT thick layer was deposited on a stainless steel tube having a 2-mm diameter by using another advantage of AD method that consists in successful deposition onto curved surfaces. The rotation speed of this ultrasonic motor ranged between 1200 and 1500 rpm for a 7-15 V drive voltage.

7.2 High-Frequency Devices Applications

With increasing CPU speed and higher communication frequencies, the surface mounting technology has reached its limit in the development of the high-frequency devices in the GHz band. The present technologies of low-temperature-cofired ceramics (LTCC) and ceramics/polymer composites are not necessarily satisfying the demands because of the degradation of material properties. To tackle the problem, highly accurate fine scale integration of the dielectric, magnetic and metallic materials are required, and further miniaturization and higher performance devices are needed. An embedded capacitor with multilayer structure in FR-4 printed circuit board, shown in Fig. 20, has been developed by depositing $BaTiO_3$ ferroelectric materials onto a Cu substrate using the AD method (Ref 63, 64). A capacitance of over 300 nF/cm^2 was achieved, being 10 times larger than the competitive technology of ceramics/polymer composite films. Thus, this technology has yielded the world top performance for a capacitor fabricated at process temperature <300 °C.

Additionally, electro magnetic interference (EMI) wave absorbers and microwave imaging sensors are currently under development. The EMI suppression properties of Fe-ferrite film prepared by the AD method on a polyimide film were studied (Ref 65). The deposition rates of Fe-ferrite composite films increased proportional to the Fe ratio of Fe-ferrite powder before deposition. The Fe-ferrite composite film with Fe:ferrite = 8:2 (weight ratio) showed a remarkable EMI mitigation characteristic for microstrip line structures in the range of 2.5-10 GHz. Fe-ferrite composite films were also applied by the AD method on flexible printed circuit (FPC), as shown in Fig. 21. The FPC was connected to a transmitter board and a receiver board. Compared with a FPC without Fe-ferrite composite films, the FPC with such a film could

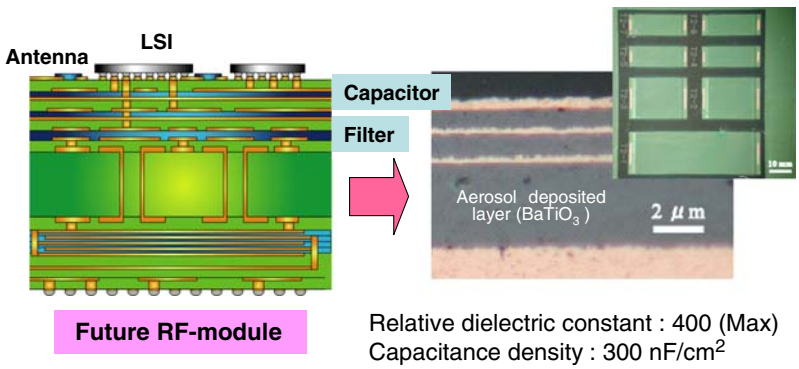

Fig. 20 Formation on thin film capacitor in FR4 resign printed circuit boards at room temperature using AD method (Ref 63)

suppress electric field intensity by about 10 dB around 1.2 GHz in the far field, which was the resonance frequency of the FPC.

7.3 Optical Devices Applications

With the anticipated requirement of ultra-high-speed integrated optical circuits to deal with the need for high-capacity information processes, the development of an ultra-high-speed optical modulator has been studied. Using the AD method, PLZT electro-optic materials have been successfully deposited onto a glass substrate at 100 °C lower than the conventional processing temperature. Transparent film was successfully obtained (Fig. 22) having an electro-optical constant (rc) of 102-168 pm/V that is two times larger than that of conventional thin films and 5-6 times larger than that of single crystal $LiNbO_3$ denoting the world's highest performance (Ref 66, 67). A Fabry-Perot typed optical modulator using this film was also fabricated. Recently, a microscopic electro-optic field probe (Ref 68) was fabricated by directly depositing a $Pb(Zr_{0.3}Ti_{0.7})O_3$ layer onto an optical fiber edge having 125 μm in diameter using the AD method, as shown in Fig. 23. An RF electro-optic signal was successfully measured over a microstrip line. The capability for GHz range fields was also shown. This device has a great potential for detailed electrical characterization in the microscopic regions of high-performance electronic products such as the interconnecting parts between LSI packages and printed circuit boards and spaces among different LSI chips in a package. In the future, the development of a high-speed optical modulator with a low-driving voltage using a ceramic film is intended for applications in a wide variety of areas such as the realization of miniaturization of network equipment and high-speed computer data transfer.

8. Summary

In this article, the high potential of AD technique on the fabrication of electro-ceramic thick films for micro-device applications has been highlighted. By comparison

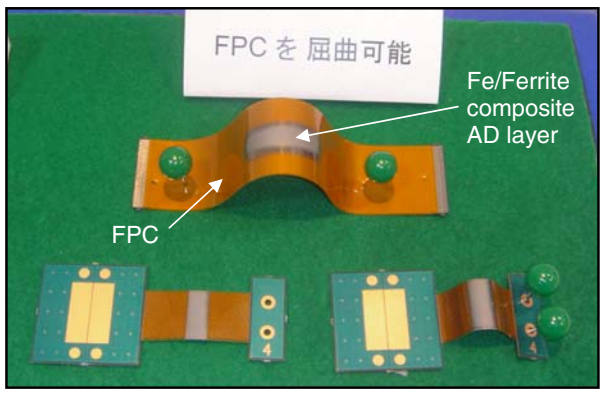

Fig. 21 EMI suppression layer (Fe/Ferrite) deposited on FPC at room temperature by AD method

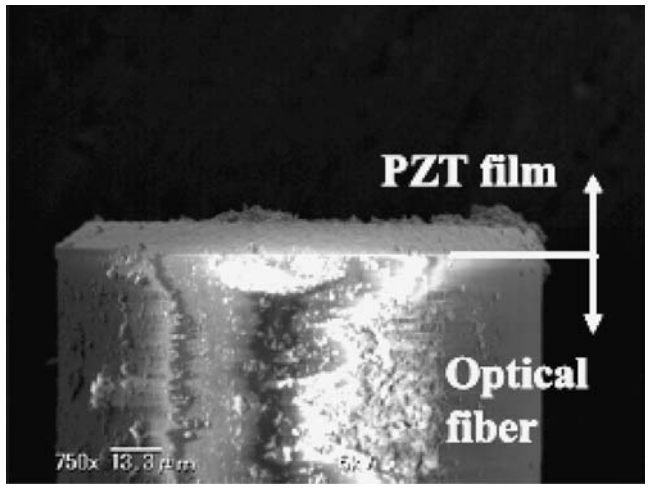

Fig. 23 SEM image of an optical fiber edge that was taken from the side after PZT film was deposited on a fiber facet (Ref 68)

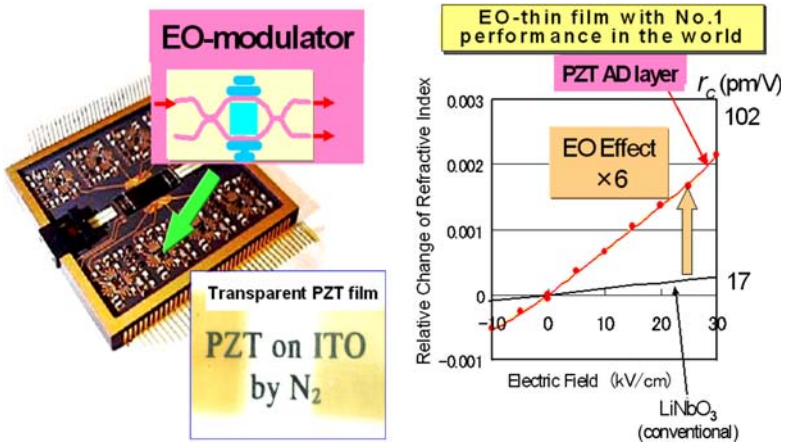

Fig. 22 Electro-optic layer directly deposited on Si structure for Si-nano-photonic devices (ultra-high-speed integrated optical circuits at 10 GHz range) by AD method, and EO constant (rc) of this layer (Ref 66)

with conventional thin-film technology and thermal spray coating processes, the AD method shows important advantages such as: (i) high-deposition rate, (ii) low-process temperature, (iii) dense film formation at a low temperature, and (iv) primary material composition and crystal structure is retained in the deposited films due to RTIC process.

For AD method, the following topics have been discussed:

1. High-speed formation of ceramic films at room temperature with high densification (over 95%) and high transparency (60-90%) is possible by deposition conditions and/or ceramic particle diameter optimizations. Film formation is possible without thermal or plasma energy assistance due to a process called RTIC. The influence of particle impact velocity, the carrier gas and starting powder properties on the deposition rate has been analyzed in an attempt to offer a reasonable explanation for the deposition mechanism. The deposition is explained by particle-substrate and particle-particle bondage due to the pressure and rise in temperature at the point of impact and particle break down during collisions.
2. Comparison of AD method with conventional thin-film technology and thermal spray-coating processes has been performed by making short descriptions of the techniques that shows similarities with AD method and revealing their minuses.
3. The electrical properties of AD films were investigated along with the effects of a heat treatment on the deposited films for α-Al_2O_3 and PZT. The AD α-Al_2O_3 films generally have a high-electrical insulation and electrical breakdown characteristics that exceed the values for the bulk material. Also, the dielectric constant and piezoelectric constant of the thermally treated (600 °C) PZT is comparable with that obtained by conventional coating methods but electrical breakdown and Young modulus have higher values than those for conventional film coating techniques.
4. Application of AD method into fabrication of electronic components has been introduced. Examples of piezoelectric, high frequency, and optical devices fabricated using AD method are shown emphasizing on the advantages offered by this technique.

The AD technique has the advantage to offer the possibility to deposit on any kind of substrate materials an array of materials in solid form.

More research is needed to clarify the deposition and recovery by annealing mechanisms and to understand the consolidation and particle-substrate and particle-particle bonding mechanisms.

Acknowledgments

The author is very grateful to Dr. M. Lebedev, to his laboratory's colleagues and to NEDO project members for their collaboration research. This research was supported in part by the NEDO Project on ''Nanostructure Forming for Advanced Ceramic Integration Technology in Japan: Nanotechnology Program.''

References

1. P. Muralt, A. Kholkin, M. Kohli, T. Maeder, K.G. Brooks, and R. Luthier, Fabrication and Characterization of PZT Thin Films for Micromotors, *Integr. Ferroelectrics*, 1995, **11**, p 213-220
2. S. Akamine, T.R. Albrecht, M.J. Zdeblick, and C.F. Quate, A Planar Process for Microfabrication of a Scanning Tunneling Microscope, *Sens. Actuat. A*, 1990, **23**, p 964-970
3. T.-A. Massood, *MICROACTUATORS: Electrical, Magnetic, Thermal, Optical, Mechanical, Chemical and Smart Structures*, H.L. Tuller, Series Ed., Kluwer Academic Publishers, 1998
4. A. Manz, N. Graber, and H.M. Widmer, Miniaturized Total Chemical Analysis Systems: A Novel Concept for Chemical Sensing, *Sens. Actuat. B*, 1990, **1**, p 244-248; P. Bergveld, *Proc. Micro Total Analysis Systems Workshop μ-TAS'94*, 1994, 1
5. S. Koganezawa, Y. Uematsu, T. Yamada, H. Nakano, J. Inoue, and T. Suzuki, Dual-stage Actuator System for Magnetic Disk Drives Using a Shear Mode Piezoelectric Microactuator, *IEEE Trans. Magn.*, 1999, **35**(2), p 988-992
6. J. Akedo and M. Lebedev, Ceramics Coating Technology based on Impact Adhesion Phenomenon with Ultrafine Particles—Aerosol Deposition Method for High Speed Coating at Low Temperature, *Materia*, 2002, **41**(7), p 459-466, in Japanese
7. M. Sayer and K. Sreenivas, Ceramic Thin Films: Fabrication and Applications, *Science*, 1990, **247**, p 1056-1060
8. I.R. Abothu, Y. Ito, P. Poosanaas, S. Kalpat, S. Komarneni, and K. Uchino, Sol-gel Processing of Piezoelectric Thin Films, *Ferroelectrics*, 1999, **232**, p 191-195
9. H.D. Chen, K.R. Udayakumar, C.J. Gaskey, L.E. Cross, J.J. Bernstein, and L.C. Niles, Fabrication and Electrical Properties of Lead Zirconate Titanate Thick Films, *J. Am. Ceram. Soc.*, 1996, **79**, p 2189-2192
10. Ph. Luginbuhl, G.-A. Racine, Ph. Lerch, B. Romanowicz, K.G. Brooks, N.F. de Rooij, Ph. Renaud, and N. Setter, Piezoelectric Cantilever Beams Actuated by PZT Sol-gel Thin Film, *Sens. Actuat. A*, 1996, **54**, p 530-535
11. S.Watanabe, T. Fujiu, and T. Fujii, Effect of Poling on Piezoelectric Properties of Lead Zirconate Titanate Thin Films Formed by Sputtering, *Appl. Phys. Lett.*, 1995, **66**, p 1481-1483
12. M. Sakata, S. Wakabayashi, M. Ikeda, H. Goto, M. Takeuchi, and T. Yada, Pb-Based Ferroelectric Thin Film Actuator for Optical Applications, *J. Microsyst. Technol.*, 1995, **2**, p 26-31
13. Y. Sakashita, T. Ono, H. Segawa, K. Tominaga, and M. Okada, Preparation and Electrical Properties of MOCVD-deposited PZT Thin Films, *J. Appl. Phys.*, 1991, **69**, p 8352-8357
14. H. Kidoh, T. Ogawa, A. Morimoto, and T. Shimizu, Ferroelectric Properties of Lead-zirconate-titanate Films Prepared by Laser Ablation, *Appl. Phys. Lett.*, 1991, **58**(25), p 2910-2912
15. M. Oikawa and K. Toda, Preparation of $Pb(Zr,Ti)O_3$ Thin Films by an Electron Beam Evaporation Technique, *Appl. Phys. Lett.*, 1976, **29**(8), p 491-492
16. R.N. Castellano and L.G. Feinstein, Ion-beam Deposition of Thin Films of Ferroelectric Lead Zirconate Titanate (PZT), *J. Appl. Phys.*, 1979, **50**(6), p 4406-4411
17. Y. Ohba, M. Miyauchi, T. Tsurumi, and M. Daimon, Analysis of Bending Displacement of Lead Zirconate Titanate Thin Film Synthesized by Hydrothermal Method, *Jpn. J. Appl. Phys.*, 1993, **32**, p 4095-4098
18. K. Shimomura, T. Tsurumi, Y. Ohba, and M. Daimon, Preparation of Lead Zirconate Titanate Thin Film by Hydrothermal Method, *Jpn. J. Appl. Phys.*, 1997, **30**, p 2174-2177
19. B. Morten, G. De Cicco, A. Gandolfi, and C. Tonelli, PZT-based Thick Films and the Development of a Piezoelectric Pressure Sensor, *Hybrid Circ.*, 1992, **28**, p 25-28
20. H.D. Chen, K.R. Udayakumar, L.E. Cross, J.J. Bernstein, and L.C. Niles, Dielectric, Ferroelectric, and Piezoelectric Properties of Lead Zirconate Titanate Thick Films on Silicon Substrates, *J. Appl. Phys.*, 1995, **77**, p 3349-3353

21. Y. Akiyama, K. Yamanaka, E. Fujisawa, and Y. Kowata, Development of Lead Zirconate Titanate Family Thick Films on Various Substrates, *Jpn. J. Appl. Phys.*, 1999, **38**, p 5524-5527
22. C.V.R. Vasant Kumar, M. Sayer, R. Pascual, D.T. Amm, and Z. Wu, Lead Zirconate Titanate Films by Rapid Thermal Processing, *Appl. Phys. Lett.*, 1991, **58**(11), p 1161-1163
23. M.R. Poor and C.B. Fledderman, Measurements of Etch Rate and Film Stoichiometry Variations During Plasma Etching of Lead-Lanthanum-Zirconium-Titanate Thin Films, *J. Appl. Phys.*, 1991, **70**, p 3385-3387
24. C.W. Chung, Reactive Ion Etching of $Pb(Zr_xTi_{1-x})O_3$ Thin Films in an Inductively Coupled Plasma, *J. Vac. Sci. Technol. B*, 1998, **16**, p 1894-1900
25. X. Li, T. Abe, and M. Esashi: Deep Reactive Ion Etching of Pyrex Glass, *Proc. IEEE MEMS'2000*, 2000, pp 271 (Miyazaki, Japan)
26. K. Saito, J.H. Choi, T. Fukuda, and M. Ohue, Reactive Ion Etching of Sputtered $PbZr_{1-x}Ti_xO_3$ Thin Films, *Jpn. J. Appl. Phys.*, 1992, **31**, p L1260-L1262
27. J. Akedo, Aerosol Deposition Method for Fabrication of Nano Crystal Ceramic Layer- Novel Ceramics Coating with Collision of Fine Powder at Room Temperature, *Mater. Sci. Form*, 2004, **449-452**, p 43-48
28. J. Akedo and M. Lebedev, Microstructure and Electrical Properties of Lead Zirconate Titanate (Pb(Zr52/Ti48)03) Thick Film Deposited with Aerosol Deposition Method, *Jpn. J. Appl. Phys.*, 1999, **38**(9B), p 5397-5401
29. J. Akedo, Aerosol Deposition of Ceramic Thick Films at Room Temperature—Densification Mechanism of Ceramic Layer, *J. Am. Ceram. Soc.*, 2006, **89**(6), p 1834-1839
30. M. Kiyohara, Y. Tsujimichi, K. Mori, H. Hatono, J. Migita, T. Kusunoki, N. Minami, M. Lebedev, and J. Akedo, *Proc. of 15th Ceram. Soc. Jpn. Autumn Symp.*, 228, 2002
31. M. Levedev, J. Akedo, K. Mori, and T. Eiju, Simple Self-Selective Method of Velocity Measurement for Particles in Impact-Based Deposition, *J. Vac. Sci. Tech. A*, 2000, **18**(2), p 563-566
32. J. Akedo and M. Lebedev, Influence of Carrier Gas Conditions on Electrical and Optical Properties of Pb(Zr,Ti)O3 Thin Films Prepared by Aerosol Deposition Method, *Jpn. J. Appl. Phys.*, 2001, **40**, p 5528-5532
33. G.R. Johnson and T.J. Holmquist, An Improved Computational Constitutive Model for Brittle Materials. High Pressure Science and Technology - 1993, Vol. 2, S.C. Schmidt, J.W. Shaner, G.A. Samara, and M. Ross, Eds., New York: AIP Press, 1994, p 981-984
34. T.J. Holmquist, G.R. Johnson, D.E. Grady, C.M. Lopatin, and E.S. Hertel, High Strain Rate Properties and Constitutive Modeling of Glass, *Proceedings of 15th International Symposium on Ballistics*, May 21-24, 1995, pp 237-244 (TB31, Jerusalem, Israel)
35. C.E. Anderson, G.R. Johnson, and T.J. Holmquist, Ballistic Experiments and Computations of Confined 99.5% Al_2O_3 Ceramic Tiles, *Proceedings of 15th International Symposium on Ballistics*, May 21-24, 1995, pp 65-72 (G6, Jerusalem, Israel)
36. H. Hirai and K. Kondo, Shock-Compacted Si_3N_4 Nanocrystalline Ceramics: Mechanisms of Consolidation and of Transition from α- to β-form, *J. Am. Ceram. Soc.*, 1994, **77**, p 487-492
37. J.J. Petrovic, B.W. Olinger, and R.B. Roof, Explosive Shock Loading on Alpha-Si_3N_4 Powder, *J. Mater. Sci.*, 1985, **20**, p 391-398
38. M. Yoshida, H. Ogiso, S. Nakano, and J. Akedo, Compression Test System for a Single Submicron Particle, *Rev. Sci. Instr.,* 2005, **76**, e-093905-1-5
39. R.C. Dykhuizen, M.F. Smith, D.L. Gilmore, R.A. Neiser, X. Jiang, and S. Sampath, Impact of High Velocity Cold Spray Particle, *J. Thermal Spray Technol.*, 1999, **8**, p 559-564
40. J. Vlcek, H. Huber, and H. Voggenreiter, Kinetic Powder Compaction Applying the Cold Spray Process—A Study on Parameter, *Proc. of ITSC2001*, 417, 2001
41. L. Scudiero, J.T. Dickinson, and Y. Enomoto, The Electrification of Flowing Gases by Mechanical Abrasion of Mineral Surfaces, *Phys. Chem. Minerals*, 1998, **25**, p 566-573
42. J. Akedo and M. Lebedev, Powder Preparation for Lead Zirconate Titanate Thick Films in Aerosol Deposition Method, *Jpn. J. Appl. Phys.*, 2002, **41**, p 6980-6984
43. M. Lebedev and J. Akedo, Patterning Properties of Lead Zirconate Titanate (PZT) Thick Films Made by Aerosol Deposition, *IEEJ Trans. Sens. Micromach.*, 2000, **120-E**(12), p 600-601
44. J. Akedo, Study on Rapid Micro-structuring using Jet-molding: Present Status and Structuring Subjects Toward HARMST, *Microsyst.Technol.*, 2000, **6**(11), p 205-209
45. T. Ide, Y. Mori, N. Ikawa, and H. Yagi, The Film Formation Method Using Hypervelocity Microparticle Impact by Electrostatic Acceleration (1st Report)—Electrodynamic Behavior of Ultra-Fine Particles during Film Growth, *J. Jpn. Soc. Prec. Eng.*, 1991, **57**, p 122-127, in Japanese
46. F. Fukuzawa, Micro Particle Ion Beam (Macron Beam), *Oyo Buturi*, 1991, **60**(7), p 720-721, in Japanese
47. P. Alkimov, V.F. Kosarev, and A.N. Papyrin, A Method of Cold Gas-Dynamic Deposition, *Dokl. Akad. Nauk SSSR*, 1990, **315**(5), p 1062-1065
48. C. Hayashi, S. Kashu, M. Oda, and F. Naruse, The Use of Nanoparticles as Coatings, *Mater. Sci. Eng. A*, 1993, **163**, p 157-161
49. T. Ide, Y. Mori, I. Konda, N. Ikawa, and H. Yagi, The Film Formation Method Using Hypervelocity Microparticle Impact by Electrostatic Acceleration (2nd Report)—Preparation of Diamond-like Carbon Film, *J. Jpn. Soc. Prec. Eng.*, 1991, **57**, p 143-148, in Japanese
50. C. Hayahi, Ultrafine Particles, *J. Vac. Sci. Technol. A*, 1987, **5**(4), p 1375-1384
51. N.P. Rao, N. Tymiak, J. Blum, A. Neuman, H.J. Lee, S.L. Girshick, P.H. McMurry, and J. Heberlein, Hypersonic Plasma Particle Deposition of Nanostructured Silicon and Silicon Carbide, *J. Aerosol. Sci.*, 1998, **29**, p 707-720
52. E. Barborini, P. Piseri, A. Podesta, and P. Milani, Cluster Beam Microfabrication of Pattern of Three-dimensional Nanostructured Objects, *Appl. Phys. Lett.*, 2000, **77**, p 1059-1061
53. J. Akedo and M. Kiyohara, Nanostructuring and Shock Compaction using Fine Particle Beam—Aeorsol Deposition for Forming of Nanocrystal Layer and Powder Technology, *J. Soc. Powder Tech.*, 2006, **43**(5), p 376-384, in Japanese
54. S.-M. Nam, M. Momotani, N. Mori, H. Kakemoto, S. Wada, J. Akedo, and T. Tsurumi, Microstrip Band Pass Filter of GHz Region Employing Aerosol-Deposited Alumina Thick Films, *Integr. Ferroelectr.*, 2004, **66**, p 301-310
55. J. Akedo, Aerosol Deposition for Coating of Transparent and High Resistive Ceramic Layer, *Metal AGNE Gijutsu Center*, 2005, **75**(3), p 16-23, in Japanese
56. J. Akedo and M. Lebedev, Piezoelectric Properties and Poling Effect of $Pb(Zr,Ti)O_3$ Thick Films Prepared for Microactuators by Aerosol Deposition, *Appl. Phys. Lett.*, 2000, **77**(11), p 1710-1712
57. J. Akedo and M. Lebedev, Effects of Annealing and Poling Conditions on Piezoelectric Properties of $Pb(Zr_{0.52},Ti_{0.48})O_3$ Thick Films Formed by Aerosol Deposition Method, *J. Cryst. Growth*, 2002, **235**, p 397-402
58. Y. Kawakami and J. Akedo, Annealing Effect on 0.5Pb(Ni1/3Nb2/3)O3-0.5Pb(Zr0.3Ti0.7)O3 Thick Film Deposited By Aerosol Deposition Method, *Jpn. J. Appl. Phys.*, 2005, **44**, p 6934-6937
59. N. Asai, R. Matsuda, M. Watanabe, H. Takayama, S. Yamada, A. Mase, M. Shikida, K. Sato, M. Lebedev, and J. Akedo, A Novel High Resolution Optical Scanner Actuated by Aerosol Deposited PZT Films. *Proc. of MEMS 2003*, 2003, p 247-250 (Kyoto, Japan)
60. J. Akedo, M. Lebedev, H. Sato, and J.H. Park, High-Speed Optical Microscanner Driven with Resonation of Lamb Waves Using Pb(Zr,Ti)O3 Thick Films Formed by Aerosol Deposition, *Jpn. J. Appl. Phys.*, 2005, **44**, p 7072-7077
61. H. Takagi, M. Mizoguchi, J.H. Park, K. Nishimura, H. Uchida, M. Lebedev, J. Akedo, and M. Inoue, PZT-Driven Micromagnetic Optical Devices, *Mat. Res. Soc. Symp. Proc.*, 2004, **785**, p D6.10.1-D6.10.6
62. Nanotech2007 NEDO project on ''Nanostructure Forming for Advanced Ceramic Integration Technology in Japan: Nanotechnology Program'' Pamphlet, 2/21, 2007

63. Y. Imanaka and J. Akedo, Integrated RF Module Produced by Aerosol Deposition Method, *Proceedings of the 54th Electronic Components and Technology Conference (ECTC)*, 2004, p 1614-1620
64. S.-M. Nam, H. Yabe, H. Kakemoto, S. Wada, T. Tsurumi, and J. Akedo, Low Temperature Fabrication of $BaTiO_3$ Thick Films by Aerosol Deposition Method and Their Electric Properties, *Trans MRS Jpn.*, 2004, **29**(4), p 1215-1218
65. S. Sugimoto K. Haga, M. Nakada, T. Kagotani, K. Inomata, and J. Akedo ''Magnetic Properties of Fe/(NiZnCu)Fe_2O_4 Composite Films Prepared by Aerosol Deposition Method,'' *INTERMAG 2005*, 2005, Nagoya, Japan, April 4-8, EC-04
66. M. Nakada, K. Ohashi, and J. Akedo, Optical and Electro-optical Properties of $Pb(Zr,Ti)O_3$ and $(Pb,La)(Zr,Ti)O_3$ Films Prepared by Aerosol Deposition Method, *J. Cryst. Growth*, 2005, **275**, p e1275-1280
67. M. Nakada, K. Ohashi, M. Lebedev, and J. Akedo, Electro-Optic Properties of $Pb(Zr1 - xTix)O_3$ (X = 0, 0.3, 0.6) Films Prepared by Aerosol Deposition, *Jpn. J. Appl. Phys.*, 2005, **44**, p L1088-L1090
68. M. Iwanami, M. Nakada, H. Tsuda, K. Ohashi, and J. Akedo, Ultra Small Electro-optic Field Probe Fabricated by Aerosol Deposition, *IEICE Electro. Express*, 2007, **4**(2), p 26-32